Journal of Sound and Vibration 333 (2014) 6651–6661

Contents lists available at ScienceDirect

Journal of Sound and Vibration

journal homepage: www.elsevier.com/locate/jsvi

Dynamic stabilization of a bistable suspension system attached to a flexible host structure for operational safety enhancement

Kai Yang [a,b], R.L. Harne [b,*], K.W. Wang [b], Hai Huang [a]

[a] School of Astronautics, Beihang University, Beijing 100191, China
[b] Department of Mechanical Engineering, University of Michigan, Ann Arbor, MI 48109-2125, USA

ARTICLE INFO

Article history:
Received 4 March 2014
Received in revised form
26 July 2014
Accepted 27 July 2014
Handling Editor: L.N. Virgin
Available online 20 August 2014

ABSTRACT

In engineering applications, a suspension system may be attached to a flexible host structure, e.g. spacecraft truss, to provide vibration isolation for sensitive instrumentation, where the suspension and host structure dynamics are strongly coupled. For linear suspensions, a resonance normally occurs adjacent to the roll-off frequency band, which significantly and detrimentally amplifies vibration transmission. To avoid the adverse resonance for operational safety enhancement, this research proposes a nonlinear bistable suspension and evaluates its performance when attached to a flexible host structure. Dynamic models of the bistable and comparable linear suspensions attached to the host structure are formulated, and steady-state responses are predicted using analytical and numerical methods. Results show that the bistable suspension can eliminate the harmful resonance via a dynamic stabilization phenomenon, and simultaneously retains the favorable isolation performance in the roll-off bandwidth as compared to the linear suspension. Series of experimental investigations support the analytical and numerical findings and help define design guidelines for operational safety improvement.

1. Introduction

The performance of sensitive instrumentation is often degraded by external disturbances. One common resolution is to employ a passive suspension system by using a linear spring and damper that provide an interface between the instrument and the adversely vibrating foundation or base [1]. The suspension that results from such configuration utilizes the classical "roll-off" bandwidth of response, corresponding to excitation frequencies above the system's resonance, and in this bandwidth minimizes vibration transmission from foundation disturbances to the suspended instrument.

In engineering applications, the suspension device employed for instrument vibration isolation may be attached or coupled to a flexible host structure (e.g. spacecraft truss). The flexible host structure may be subjected to harmonic vibration induced by cryogenic coolers, reaction wheels, or ground motions, to name a few common sources of vibration excitation. In many practical situations, the combination of the suspension, its load, and the host structure dynamics together can be approximately represented by a coupled two-degree-of-freedom (2dof) system [2]. This 2dof coupled system introduces two resonant features, and the second resonance occurs adjacent to the roll-off frequency band that provides useful vibration

* Corresponding author.
E-mail address: rharne@umich.edu (R.L. Harne).

http://dx.doi.org/10.1016/j.jsv.2014.07.033
0022-460X/

attenuation [2]. In practice, due to design uncertainties and changing excitation conditions, the suspension may not always be operated in the roll-off frequency band. When the excitation frequency shifts downward and approaches the resonance bandwidth, the vibration transmission may be significantly amplified by the resonance feature. It is well-known that increasing the suspension damping is ineffective to attenuate or avoid such adverse resonance, but instead significantly deteriorates isolation performance in the roll-off bandwidth [2].

To avoid the detrimental resonance and provide overall operational safety enhancement without compromising the favorable vibration isolation in the roll-off bandwidth, active and semi-active suspension alternatives have been explored [3–6]. To reduce power requirements of such systems, self-powered dampers have been proposed which electromechanically convert the disturbance vibration energy to serve as a practical energy source for the isolator [7–9]. However, externally- and self-powered suspensions commonly require numerous operating hardware, including transducers, sensors, and controllers, increasing the complexity of design, implementation, and maintenance. Therefore, *passive* suspensions, which do not require additional hardware for their implementation, are more desirable in terms of simplified and practical implementation.

An alternative method to passively enhance suspension operational safety is the incorporation of nonlinear elements, such as bistable springs. Prior studies using this approach found that the bistable spring possesses negative linear and positive cubic stiffnesses, and employed the bistable spring in parallel with a linear spring to constitute the interface of a single degree-of-freedom (sdof) isolation system [10,11]. Due to parallel combination of the bistable spring negative linear stiffness and the linear spring positive stiffness, the isolation systems were configured to achieve low, but positive, dynamic stiffness leading to increased vibration attenuation. Simultaneously, the cubic nonlinear stiffness of the bistable spring ensured small static deflection due to the suspended load [10,11].

Other recently explored characteristics of the bistable spring indicate potential for improved reduction of vibration transmission should the bistable interface be used on its own, in other words without additional parallel interface elements. A suspended load having a bistable spring interface to a moving rigid foundation realizes bistability, and is therefore a statically and dynamically sdof bistable system under base excitation. When excited periodically, a sdof bistable system exhibits two distinct steady-state behaviors: inter-well oscillation where the oscillator symmetrically vibrates about the unstable equilibrium, and intra-well oscillation where it vibrates around either stable equilibrium [12]. Two forms of inter-well response are further possible, including a large-amplitude dynamic and another response termed “excitation induced stability” (EIS) or “dynamic stabilization.” Recently, EIS was experimentally investigated by Kim et al. [13] and Wu et al. [14] using electrical and mechanical oscillators, respectively. The investigations showed that the excited bistable system may vibrate such that its *absolute* vibration is negligible leading to an apparent stationary configuration of the inertial mass. In the context of vibration isolation, the unique *dynamic stabilization* feature appears highly desirable to achieve very small absolute motion of a suspended load when the foundation vibrates periodically. Methods to maintain EIS were described and experimentally validated with a mechanical system by Wu et al. [14].

2. Research objectives and problem statement

In this research, a new concept is developed to exploit the unique characteristics of the bistable suspension and its EIS feature to significantly reduce the detrimental resonant effect near the suspension roll-off bandwidth of the combined payload-suspension-host structure dynamics as described above. However, for the strongly coupled system composed of a bistable suspension and flexible host structure in this work, the direct use of the prior methods [14] to realize dynamic stabilization phenomena is not applicable. Therefore, the dynamic stabilization feature for suspension operational safety enhancement in the 2dof coupled system must be carefully investigated.

Recently, a similar performance improvement of 2dof force transmissibility isolation was corroborated by the authors' work [15]. In that study, a bistable dual-stage isolator composed of two mass elements was designed to attenuate transmissibility passed from an *excitation force* imposed on the first (bistable) stage mass to a rigid foundation. In contrast to the previous work [15], the aim of the present study is *base excitation* suspension enhancement, which represents the reversed isolation path compared to the prior force transmissibility study and only one mass element is in the suspension assembly. Due to the inherent strong nonlinearity, a change of excitation transmission path would lead to significantly distinct dynamic behaviors and the present focus of performance improvement for frequencies adjacent to the roll-off bandwidth represent unresolved challenges as compared to the authors' previous work [15]. Therefore, in summary, this research seeks to investigate the unexplored potential for a bistable suspension when attached to a flexible host structure, to enhance operational safety by harnessing the dynamic stabilization phenomenon.

The following sections describe the development and evaluation of the bistable suspension attached to a flexible host structure. The host structure is modeled as a sdof system which is appropriate in light of targeting a single structural modal response near the suspension operating bandwidth. Models of the 2dof nonlinear coupled system are formulated and the method of harmonic balance is utilized to analytically predict the dynamics. Results are presented of comprehensive analytical, numerical, and experimental efforts that evaluate the system's performance as compared to utilizing a linear suspension. Through these studies, useful guidelines are derived for the effective implementation of such a bistable suspension and greatest assurance of operational safety enhancement.

3. Governing equations

Fig. 1 presents a schematic of the 2dof coupled system where a bistable suspension is attached to a sdof host system. Each body is modeled using lumped inertial, damping, and stiffness elements to represent the principal and often dominant vibrations characteristics of the coupled system. The bistable suspension interface suspends a mass m_1, which may represent a sensitive instrument. The bistable interface comprises a damper with damping constant d_1 and a spring with stiffness k_0 having undeformed length l_0. One end of the spring suspends the mass m_1, while the opposing end connects to a frame mounted to the flexible host structure. With respect to the motion of the suspended mass, the height of the frame is h, where $h < l_0$. Hence the spring of stiffness k_0 is compressed in the upright position and induces two stable equilibria, positioned symmetrically about a central, unstable configuration.

The host structure is modeled as a sdof linear oscillator, and its mass including the supporting frame is m_2. The stiffness and damping of the host structure are k_2 and d_2, respectively. When the 2dof nonlinear coupled system is subjected to harmonic base acceleration excitation $\ddot{z} = A\ \cos\ \Omega\tau$, the governing equations are derived as

$$m_1(\ddot{X}_\tau + \ddot{Y}_\tau + A\ \cos\ \Omega\tau) + d_1\dot{X}_\tau + F_p = 0 \tag{1}$$

$$m_2(\ddot{Y}_\tau + A\ \cos\ \Omega\tau) + d_2\dot{Y}_\tau + k_2 Y_\tau - d_1\dot{X}_\tau - F_p = 0 \tag{2}$$

$$F_p = k_0 X_\tau \left(1 - \frac{l_0}{\sqrt{{X_\tau}^2 + h^2}}\right) \tag{3}$$

where A, Ω and τ are the excitation amplitude, frequency and time. X_τ and Y_τ are the relative oscillations of the suspended mass and host structure mass, respectively, and F_p is the potential force of the bistable interface. From Eq. (3), it is seen that the bistable interface induces two stable configurations for the suspended mass relative to the frame: $X_\tau^* = \pm\sqrt{l_0^2 - h^2}$. The governing equations may be simplified by utilizing a Taylor series expansion of F_p with respect to X_τ and reserving terms up to the third order. Eqs. (1) and (2) are then simplified to be

$$m_1(\ddot{X}_\tau + \ddot{Y}_\tau + A\ \cos\ \Omega\tau) + d_1\dot{X}_\tau - k_1 X_\tau + k_3 {X_\tau}^3 = 0 \tag{4}$$

$$m_2(\ddot{Y}_\tau + A\ \cos\ \Omega\tau) + d_2\dot{Y}_\tau + k_2 Y_\tau - d_1\dot{X}_\tau + k_1 X_\tau - k_3 {X_\tau}^3 = 0 \tag{5}$$

where the simplified bistable spring has a negative linear stiffness $-k_1 = -k_0(l_0/h - 1)$ and positive cubic stiffness $k_3 = k_0 l_0/2h^3$. When suspending the mass m_1, the simplified bistable suspension has a linear resonant frequency $\omega_1 = \sqrt{k_1/m_1}$, loss factor $\gamma_1 = d_1/m_1\omega_1$, and produces two symmetric equilibria

$$X_{\text{eq}} = \pm\sqrt{k_1/k_3} = \pm\sqrt{(2l_0h^2 - 2h^3)/l_0} \tag{6}$$

bounding an unstable equilibrium at $X = 0$. In absence of the bistable interface and supported mass, the host structure has a natural frequency $\omega_2 = \sqrt{k_2/m_2}$, and its loss factor is $\gamma_2 = d_1/m_1\omega_1$. Additional non-dimensional parameters are defined, including frequency tuning ratio between the bistable suspension and the host structure $f = \omega_1/\omega_2$, mass ratio between the suspended mass and the host structure mass $\mu = m_1/m_2$, normalized excitation frequency $\omega = \Omega/\omega_2$ and time $t = \omega_2\tau$. Using these variables, a non-dimensional form of Eqs. (4) and (5) yields

$$x'' + y'' + p_0\ \cos\ \omega t + \gamma_1 f x' - f^2 x + f^2 x^3 = 0 \tag{7}$$

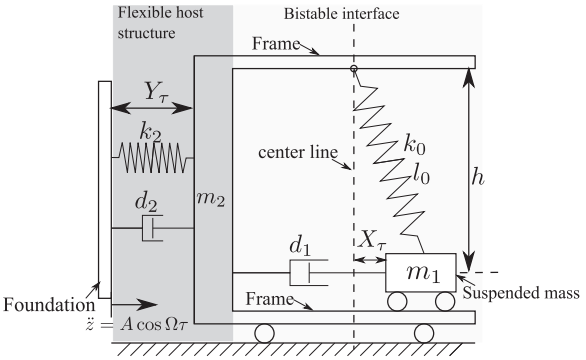

Fig. 1. Schematic of the 2dof coupled system where a bistable suspension is attached to a flexible host structure.

$$y''+p_0\ \cos\ \omega t+\gamma_2 y'+y-\mu\gamma_1 f x'+\mu f^2 x-\mu f^2 x^3=0 \tag{8}$$

where $p_0=A/|X_{eq}|\omega_2^2$; $x=X_\tau/|X_{eq}|$; $y=Y_\tau/|X_{eq}|$; and $(\ )'$ is derivative with respect to time t.

Transmissibility from the base excitation to the absolute acceleration of the suspended mass m_1 is the index to evaluate the vibration transmission attenuation of the 2dof nonlinear coupled system. Assuming single frequency sinusoidal excitation, the transmissibility is defined by the frequency response function (FRF) of the absolute acceleration of the suspended mass to the exciting acceleration:

$$|T|=\frac{\left|\ddot{X}_\tau+\ddot{Y}_\tau+A\ \cos\ \Omega\tau\right|}{|A\ \cos\ \Omega\tau|}=\frac{|x''+y''+p_0\ \cos\ \omega t|}{p_0} \tag{9}$$

4. Analytical solution method

Systems exhibiting bistability are strongly nonlinear and require appropriate analytical tools which do not rely on assumption of small perturbations about a linear response. When it is anticipated that the system undergoes periodic response in consequence to sinusoidal excitation, an effective method to analytically predict steady-state dynamic behaviors of a strongly nonlinear system is the method of harmonic balance [15–19]. In this study, a fundamental Fourier series expansion is employed to predict the steady-state response of the suspended mass and host structure mass relative oscillations, x and y, respectively.

$$x=c_1(t)+a_1(t)\sin\ \omega t+b_1(t)\cos\ \omega t \tag{10}$$

$$y=a_2(t)\sin\ \omega t+b_2(t)\cos\ \omega t \tag{11}$$

In Eq. (10), $c_1(t)=0$ indicates the suspended mass oscillates symmetrically about the unstable equilibrium induced by the bistable interface at $x=0$, i.e. an inter-well response. In contrast, $c_1(t)\neq 0$ represents an intra-well response where the suspended mass has non-zero displacement away from the central configuration and undergoes vibrations about this stable equilibrium. The moduli $r_1=\sqrt{a_1^2+b_1^2}$ and $r_2=\sqrt{a_2^2+b_2^2}$ are the oscillation amplitudes of x and y.

Substituting Eqs. (10) and (11) into Eqs. (7) and (8), five modulation equations with respect to the coefficients $\mathbf{q}=[c_1\ a_1\ b_1\ a_2\ b_2]^T$ are obtained. Then, by assuming steady-state response and reducing the set of equations through incremental substitution, a polynomial is obtained whose roots represent the amplitude squared r_1^2 of the suspended mass connected to the bistable interface

$$r_1^2(\alpha_1\Lambda^2+\alpha_2\Lambda+\alpha_3)=(1+\omega^2\gamma_2^2)p_0^2 \tag{12}$$

where

$$\Lambda=-1+3c_1^2+\tfrac{3}{4}r_1^2 \tag{13a}$$

$$\alpha_1=[f^2-(1+\mu)f^2\omega^2]^2+(f^2\omega\gamma_2)^2 \tag{13b}$$

$$\alpha_2=-2f^2\omega^2\{(1-\omega^2)[1-(1+\mu)\omega^2]+(\omega\gamma_2)^2\} \tag{13c}$$

$$\begin{aligned}\alpha_3=&\omega^2\{(1-\omega^2)^2\omega^2+(f\gamma_1)^2[1-(1+\mu)\omega^2]^2\\&+\omega^2[(f\gamma_1\gamma_2)^2+(\omega\gamma_2)^2+2\mu f\gamma_1\gamma_2\omega^2]\}\end{aligned} \tag{13d}$$

One of the modulation equations with respect to coefficient set $\mathbf{q}$ has two distinct solutions for c_1^2. The solutions satisfy $c_1^2=0$ for inter-well oscillations and $c_1^2=1-(3/2)r_1^2$ for intra-well oscillations. By substituting a potential solution for c_1^2 into Eqs. (12) and (13), the roots of the polynomial Eq. (12) are then computed, and the coefficient set $\mathbf{q}$ is incrementally back-calculated [19]. The negative real components of the eigenvalues of the Jacobian matrix of the modulation equations indicates stability of a given response coefficient set. In this manner, the physically meaningful and stable responses of the system are predicted.

Therefore, the analytical results of the transmissibility $|T|$ are expressed by

$$|T|=\frac{\sqrt{(a_1+a_2)^2\omega^4+(b_1\omega^2+b_2\omega^2-p_0)^2}}{p_0} \tag{14}$$

5. Description of the linear suspension for comparison

In this section, a counterpart linear suspension is defined for performance comparison when attached to the sdof host structure. For meaningful comparison, we require that both the bistable and linear suspensions provide identical isolation performance in the

roll-off frequency band. Because vibration from the foundation may be highly attenuated in the roll-off frequency band, the suspension oscillation may be small. When a nonlinear system undergoes small oscillations, the nonlinearity can be neglected so that its response is nearly identical to that of a linearized counterpart [16]. Therefore, the counterpart linear suspension is defined from a linearization of the bistable suspension characteristics. When the bistable suspension exhibits small oscillations, the suspended mass m_1 vibrates around either stable equilibrium: the intra-well response. The response motion may then be expressed by $X_\tau = \delta x \pm \sqrt{l_0^2 - h^2}$, where $\delta x \ll l_0$. Hence, the potential force of the bistable interface becomes

$$F_p = k_0\left(\delta x \pm \sqrt{l_0^2 - h^2}\right)\left(1 - \frac{l_0}{\sqrt{\delta x^2 \pm 2\delta x\sqrt{l_0^2 - h^2} + l_0^2}}\right) \tag{15}$$

After Taylor expansion of Eq. (15) with respect to the small quantity $\delta x/l_0$, and neglecting the higher order, a linear expression of Eq. (15) is found to be

$$F_p \approx k_0\left(1 - \frac{h^2}{l_0^2}\right)\delta x = Lk_1\delta x \tag{16}$$

where

$$L = \left(1 - \frac{h^2}{l_0^2}\right)/\left(\frac{l_0}{h} - 1\right) \tag{17}$$

Eq. (16) defines a linearized restoring force of the bistable suspension. Thus, the linear counterpart is realized with a linear interface composed of damping d_1 and stiffness Lk_1, the latter following from the expression in Eq. (16). In this way, the linear counterpart serves as the benchmark for meaningful comparison against the bistable suspension. The additional non-dimensional parameters of interest for the corresponding 2dof linear coupled system are the frequency tuning ratio $f_l = \sqrt{L}f$, and loss factor of the linear counterpart $\gamma_{l1} = \gamma_1/\sqrt{L}$.

6. Numerical and analytical results

The governing equations of the 2dof coupled systems are first evaluated by comparing a series of numerical and analytical results, to provide for model validation as well as investigate the difference in vibration transmission achieved by the bistable and linear suspensions. For the following numerical simulations, the original length of the spring in the bistable interface is l_0=0.08 m, and the ratio between the frame height and the original spring length is h/l_0=0.99. Therefore, according to Eqs. (3) and (6), providing the bistable interface restoring forces before and after Taylor series expansion, the stable equilibria of the original and simplified bistable interface are $\pm$0.0113 m and $\pm$0.0112 m, respectively. The mass ratio and frequency tuning ratio from the bistable suspension to the host structure are μ=0.34 and f=0.28, respectively. The bistable suspension loss factor is $\gamma_1 = 0.15$, while the host structure has a small loss factor $\gamma_2 = 0.03$. For the counterpart linear suspension, the mass ratio is $\mu = 0.34$, whereas the frequency tuning ratio and loss factor are $f_l = \sqrt{L}f = 0.39$ and $\gamma_{l1} = \gamma_1/\sqrt{L} = 0.107$, respectively. The normalized amplitude of the excitation is $p_0 = 0.06$ in the following simulations.

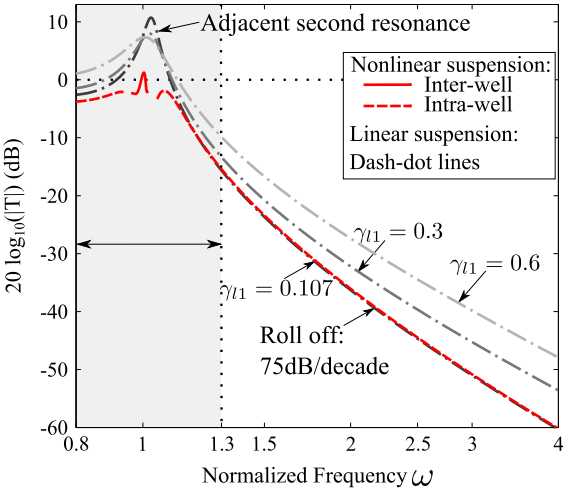

Fig. 2. Analytically predicted transmissibility $|T|$ of the 2dof coupled systems with the bistable and linear suspensions in bandwidth $0.8 \le \omega \le 4$.

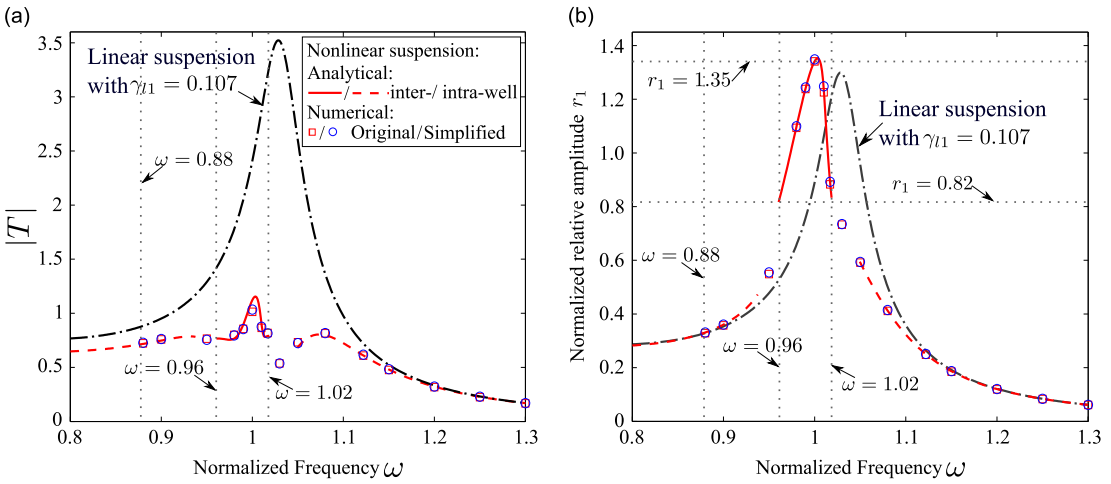

Fig. 3. (a) Transmissibility $|T|$ and (b) normalized suspension relative amplitudes $\boldsymbol{r}_1$ of the 2dof coupled systems with the bistable and linear suspensions in bandwidth $0.8 \le \omega \le 1.3$.

Fig. 2 presents analytically predicted transmissibility of the 2dof coupled systems across a wide frequency band $0.8 \le \omega \le 4$ which encompasses the roll-off frequency band and the adjacent second resonance induced by the linear coupled system. The responses of the linear coupled system are shown as the dash–dot curve, whereas responses corresponding to employment of the bistable suspension are solid or dashed curves, depending on the response form. Apart from the results of the linear counterpart with the equivalent loss factor, the figure also shows the responses when applying the linear suspensions with two other loss factors: $\gamma_{l1} = 0.3$ and $\gamma_{l1} = 0.6$, so as to evaluate whether increased linear suspension damping could be helpful for improving operational safety. In the roll-off frequency band, the nonlinear and the linear suspensions realize the same isolation performance of 75 dB/decade transmissibility attenuation rate, which provides favorable isolation performance when the suspensions are operated in this bandwidth. However, it is seen that the second resonance induced by the 2dof coupled system with the linear suspension significantly amplifies the vibration transmission across a fairly wide bandwidth around $\omega = 1$ adjacent to the roll-off frequency band. In practice, the suspension cannot always be ensured to be operated in the favorable isolation bandwidth due to common shifts in excitation frequency away from the roll-off bandwidth; the resulting amplified vibration transmission may be detrimental to the operational safety of the suspension, which may lead to failure of the suspended instrument. Therefore, this resonance should be reduced or avoided altogether. As has been shown in prior studies [2], Fig. 2 shows that increasing linear suspension damping is ineffective to reduce or avoid the detrimental resonance, and has the undesirable consequence of increasing vibration transmission in the roll-off bandwidth. In contrast, when the bistable suspension is applied, the dramatic resonance feature is substantially avoided in the resonance bandwidth; in other words, the nonlinear coupled system simply does not exhibit a substantial second resonance around excitation frequency $\omega = 1$. This enhances operational safety enhancement while simultaneously retains favorable isolation performance in the roll-off frequency band.

To more closely study the suspension performance improvement of the bistable suspension, Fig. 3 focuses on the results of Fig. 2 specifically in the shaded bandwidth $0.8 \le \omega \le 1.3$ which encompasses the conventional resonance bandwidth of the 2dof coupled system with linear suspensions. Fig. 3(a and b) present the transmissibility $|T|$ and normalized suspended mass relative amplitude r_1 of the 2dof coupled system with the bistable and linear suspensions across the shaded bandwidth, respectively. In these results, the linear counterpart employs the equivalent loss factor $\gamma_{l1} = 0.107$. To thoroughly verify the analytical results, numerical responses of the coupled system with the bistable suspension are obtained by numerically integrating the original governing Eqs. (1) and (2) as well as the Eqs. (4) and (5) following Taylor series expansion. A fourth order Runge–Kutta algorithm is employed in MATLAB to acquire the numerical results.

In the bandwidth $0.96 \le \omega < 1.02$, the analytically predicted responses of the coupled system with the bistable suspension indicate the suspended mass undergoes *inter-well oscillation*, where it vibrates symmetrically about the central unstable equilibrium. For frequencies outside of this bandwidth, the responses trend to *intra-well* response, in which case the suspended mass oscillates around one of the stable equilibria. In the inter-well bandwidth $0.96 \le \omega < 1.02$, Fig. 3(b) shows that the relative oscillation amplitude of the bistable suspension is $0.82 \le r_1 \le 1.35$, which is close to the value of the normalized stable equilibrium amplitude of the bistable interface $r_1^* = 1$. As a result, the inter-well response is termed *excitation induced stability* (EIS) [14]—the dynamic stabilization phenomenon—which is characteristically defined by small symmetric oscillations of a bistable system around its unstable configuration. As shown in Fig. 3(a), the 2dof coupled system with the linear suspension has a resonance that greatly amplifies the vibration transmitted to the suspended mass in the vicinity of $\omega = 1$ which is adjacent to the roll-off frequency band. In contrast, in the EIS frequency band $0.96 \le \omega < 1.02$, the maximum transmissibility of the coupled system with the bistable suspension is much smaller than the linear counterpart, showing that using the bistable suspension avoids the detrimental resonance with comparable magnitude induced by the

2dof linear coupled system. Fig. 3(b) finds that the maximum bistable suspension oscillation is similar to that of the linear counterpart, indicating that the improved performance by means of the bistable suspension does not come at the cost of requiring greater dynamic stroke range.

Fig. 3(a andb) also present results of numerically integrating both the original governing Eqs. (1) and (2) and simplified Eqs. (4) and (5) by squares and circles, respectively. The numerical results are obtained from the time series simulations by calculating maximum amplitudes of steady-state single periodic responses. Both numerical results have good agreement with the analytical findings, validating the model composition and demonstration that simplification of governing equations does not reduce fidelity of the model formulation. In the bandwidth $0.8 \le \omega < 0.88$, numerical simulations predict multi-harmonic responses may occur depending on initial conditions. The maximum amplitude of the multi-harmonic response at each excitation frequency is greater than the analytically predicted single periodic response, and thus the multi-harmonic response is not desired. Note that the normalized excitation frequency in Fig. 3(a and b) is relative to the natural frequency of the host structure $\omega_2 = \sqrt{k_2/m_2}$. Thus in practice, by designing appropriate parameters, the undesirable multi-harmonic responses might be outside of the operating bandwidth, so that the system exhibits only the single periodic response in the bandwidth of operation. Since the present study is focused on the single periodic response that is conducive to operational safety enhancement, the multi-harmonic results are omitted in the figures.

7. Influences of excitation conditions

Unlike the 2dof coupled system with the linear suspension, the transmissibility of the coupled system with the bistable suspension is dependent on excitation level. To evaluate this sensitivity as normalized excitation level varies from $0.001 \le p_0 \le 0.1$, Fig. 4(a) presents a contour map of the analytically predicted single periodic transmissibility of the coupled system with the bistable suspension across the bandwidth $0.8 \le \omega \le 1.3$. Three response regions are shown, each defined within the bounds of the red dashed curves, which represent the stable inter- and intra-well responses, and the unstable (unshaded) solutions. In the map, darker shading indicates increased transmissibility. When $p_0 \le 0.035$, the system does not exhibit inter-well response across the bandwidth. When $p_0 > 0.035$, the inter-well response emerges in the vicinity of $\omega = 1$, and the inter-well bandwidth is widened by increasing the excitation level p_0. As shown in the contour map, the green solid line presents the transmissibility *maxima* for each level of excitation, and it is seen that the transmissibility maxima are all in the vicinity of $\omega = 1$. The transmissibility maxima indicate the maximum vibration transmission amplification under respective excitation levels in the bandwidth that is the worst case for the suspension operational safety. Therefore, the smaller the value obtained, the better the suspension performance. Following the green solid line of maximum transmissibility, it is found that moderate excitation levels suppress the maxima.

For clarity, Fig. 4(b) plots the transmissibility maxima indicated by the green solid line in Fig. 4(a). The transmissibility maxima of the 2dof coupled system with the linear suspension across the excitation level range $0.001 \le p_0 \le 0.1$ in the same bandwidth are also provided. As anticipated, the transmissibility of the 2dof linear coupled system does not vary as excitation level is changed. However, the transmissibility when using the bistable suspension exhibits a minimum across the range of excitation considered. It is seen that the transmitted vibration with the bistable suspension is minimized for moderate excitation level $p_0 \approx 0.05$. This feature indicates that the bistable suspension could provide greatest vibration isolation safety when the coupled system is subjected to moderate excitation level. Numerical results in Fig. 4(b) agree with the analytical findings, validating the viability of the bistable suspension for suspension operational safety enhancement.

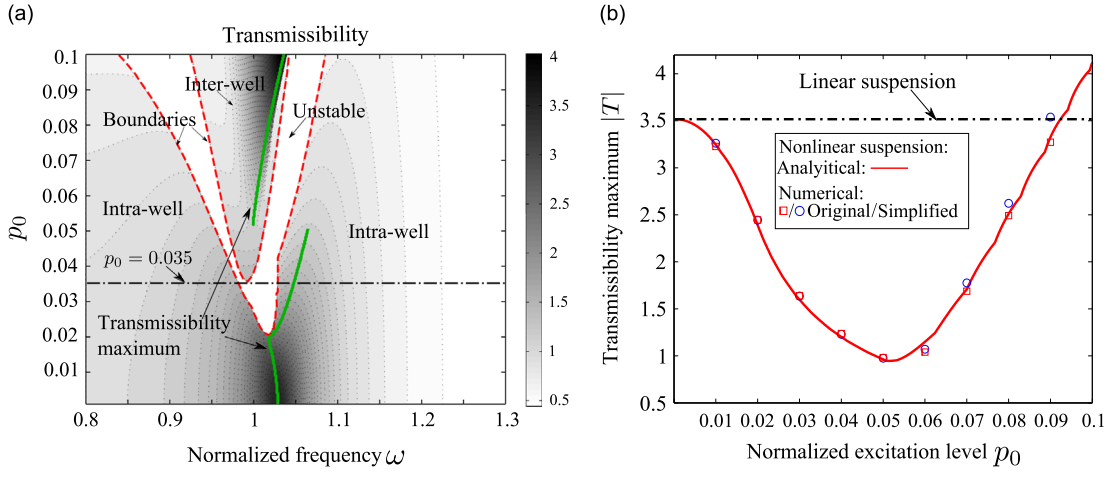

Fig. 4. (a) Transmissibility contour map of the 2dof coupled system with the bistable suspension and (b) the transmissibility maximum $|T|$ corresponding to variation of normalized excitation level p_0.

The trend of minimized transmissibility provided by the bistable suspension may be explained by the normalized potential force of the bistable interface as shown in Eqs. (7) and (8), i.e. $f^2(-x+x^3)$. Accordingly Eqs. (7) and (9), can be rewritten as follows:

$$|T| = \frac{|\gamma_1 f x' + f_p|}{p_0} \tag{18}$$

where

$$f_p = f^2(-x+x^3) \tag{19}$$

As shown in Eqs. (18) and (19), the transmissibility $|T|$ is affected by the normalized damping force $\gamma_1 f x'$ and potential force f_p. When the bistable suspension exhibits EIS under a specific excitation level, the normalized relative oscillation amplitude $r_1 = |x|$ is in the vicinity of the normalized equilibrium value $r_1^* = |x_{eq}| = 1$, and thus the positive nonlinear force $f^2 x^3$ may counterbalance the negative linear force $-f^2 x$ so that the transmissibility is minimized as shown in Fig. 4(b), which helps to avoid detrimental vibration amplification in the resonance bandwidth.

Note that the normalized excitation level is defined as $p_0 = A/|X_{eq}|\omega_2^2$, where the equilibrium of the simplified bistable interface X_{eq} is related to the undeformed spring length l_0 and frame height h. Therefore, if the excitation level A and natural frequency of the host structure ω_2 are known, the optimal suspension safety may be achieved by properly selecting the spring length l_0 and height h.

8. Experimental and analytical parametric study

A prototype of the bistable suspension is fabricated, and the 2dof coupled system with the bistable suspension attached to a sdof flexible host structure is constructed. A series of experimental investigations are performed to demonstrate the important suspension characteristics uncovered in Section 5 and to further validate the analytical model through qualitative comparison with measured data.

8.1. Experiment setup

Fig. 5 shows the experimental setup. The 2dof nonlinear coupled system is attached to an electrodynamic shaker which provides harmonic base acceleration. The bistable suspension interface consists of a spring compressed in its upright vertical position and an adjustable damper. Between two rotational bearings, the spring connects the surrounding frame to the suspended mass, which is the top bearing and rotational bearing attached to it. The spring is initially compressed when the top bearing is aligned with the center line. In this way the bistable suspension induces two stable equilibria symmetric about the center line. The frame is mounted on the bottom bearing and is connected to the shaker by a spring providing the sdof host structure stiffness.

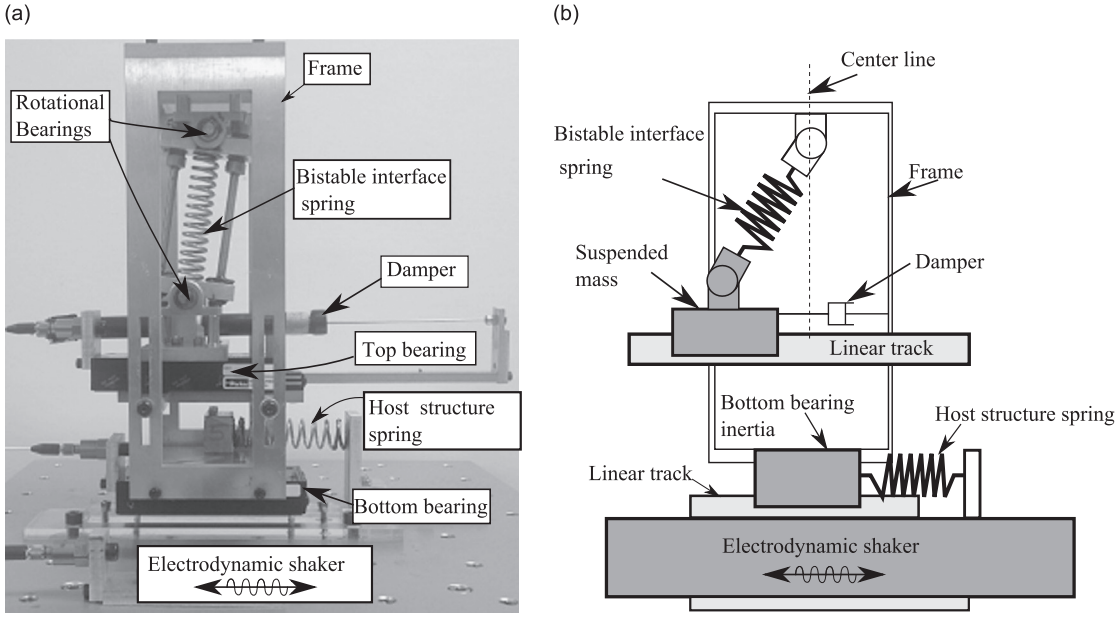

Fig. 5. Experimental setup: (a) photograph and (b) schematic.

The combined mass of the top bearing and rotational bearing connected to it represents the suspended mass $m_1 = 0.347$. The total mass of the frame, bottom bearing, and other hardware rigidly attached to the frame represents the host structure mass $m_2 = 1.029$. The linear frequency of the bistable suspension with respect to the suspended mass is $\omega_1 \approx 10.56$ rad/s (1.68 Hz) and the stable equilibria are ± 0.012 m, while the natural frequency of the host structure is $\omega_2 \approx 37.70$ rad/s (6 Hz). The shaker provides slowly backward swept sinusoidal base acceleration from 4.8 Hz to 7.8 Hz at a rate 0.025 Hz/s, and the bandwidth encompasses the resonance bandwidth of the 2dof coupled system with the linear suspension, which is adjacent to the roll-off frequency band. Two accelerometers are mounted on the shaker and the suspended mass, which provide suitable data to determine the transmission of vibration from the shaker to the suspended mass m_1.

8.2. Experimental and analytical comparisons of isolation performance

8.2.1. Excitation level variation

Three excitation levels are chosen, and their root mean squares (RMS) during the entire swept frequency band are $[A^{(1)}, A^{(2)}, A^{(3)}] = [1.02,\ 1.66,\ 2.37]\ m/s^2$. For the analytical predictions, the steady-state excitation amplitudes are $[A^{(1)}, A^{(2)}, A^{(3)}] = [0.61, 1.02, 1.43]\ m/s^2$ (i.e. the normalized amplitudes are: [0.036, 0.06, 0.084]). In the following experiments, the mass ratio and frequency tuning ratio are $\mu \approx 0.34$ and $f \approx 0.28$, respectively. Other parameters used in analyses are the same as those used to generate Fig. 2.

Fig. 6(a and b) present experimental and analytical transmissibilities $|T|$, respectively, as excitation level is varied. The horizontal axis shows the excitation frequency normalized by the natural frequency of the host structure. For the experimental results, when the smallest excitation level $A^{(1)}$ is used, the bistable suspension only exhibits intra-well response (unfilled data points) across the entire bandwidth. By increasing excitation level to $A^{(2)}$, inter-well response (filled

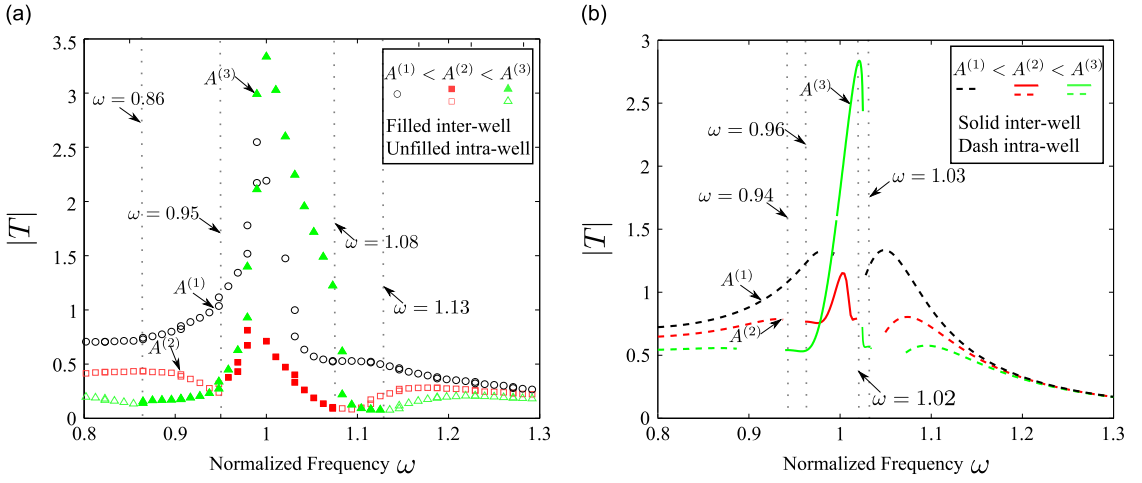

Fig. 6. (a) Experimental and (b) analytical transmissibility $|T|$ corresponding to excitation level variation.

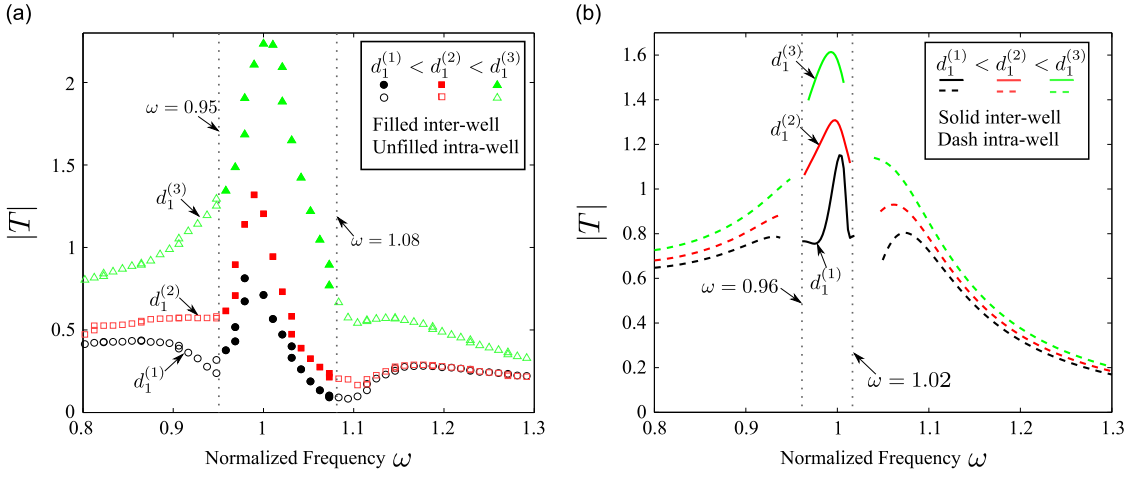

Fig. 7. (a) Experimental and (b) analytical transmissibility $|T|$ corresponding to variation of bistable suspension damping.

data points) appears throughout $0.95 \le \omega \le 1.08$, and the maximum of $|T|$ is decreased. When excitation level is further increased, the inter-well frequency bandwidth is widened to be $0.86 \le \omega \le 1.13$, and the maximum of $|T|$ is increased. Similar to the discovery in Fig. 4(a and b), the experimental results demonstrate that moderate levels of excitation lead to minimized transmissibility in the resonance bandwidth which enhances overall operational safety of the suspension system. There is a strong agreement between experimental and analytical results in Fig. 6(a and b) across the several salient trends helping to support the main conclusions regarding excitation level dependence of the bistable suspension performance when attached to the host structure.

8.2.2. Bistable suspension damping variation

The influence of the bistable suspension damping is then considered. The adjustable damper is used with three settings denoted by $d_1^{(1)}$, $d_1^{(2)}$, and $d_1^{(3)}$. Due to the frequencies involved and test apparatus available, there is difficulty in precisely identifying the damper constants for the three settings; however, the general trend is such that $d_1^{(1)} < d_1^{(2)} < d_1^{(3)}$. The RMS of excitation level in the experiment is $A = 1.66$ m/s^2, which is the moderate excitation as used for the prior experiments. For the comparable analytical results, damping constants are $[d_1^{(1)}, d_1^{(2)}, d_1^{(3)}] = [0.55, 0.92, 1.28]$ N s/m (i.e. the loss factors are: [0.15, 0.25, 0.35]), and the moderate excitation level is $A = 1.02\ m/s^2$. The mass and frequency tuning ratios remain the same as in the prior experiment set.

In the experiments, the bistable suspension exhibits inter-well response in $0.95 \le \omega \le 1.08$, as shown in Fig. 7(a), and the inter-well frequency bandwidth is observed to be mostly insensitive to damping variation. This finding is in very good agreement with the analytical results shown in Fig. 7(b). Both experimental and analytical findings indicate transmissibility is reduced as damping is reduced, suggesting this design change is one way to avoid vibration amplification around the resonance peak bandwidth. Because the bistable suspension is a strongly nonlinear system, too small damping may increase the activation likelihood of undesirable multi-harmonic or chaotic responses. From this perspective, achieving robustness in suspension performance suggests selection of moderate damping: appropriately small bistable interface damping to adequately enhance the operational safety, but not too small to activate undesired responses.

8.2.3. Variation of the suspended mass

A final critical factor to evaluate is the performance variation induced by changes in the suspended mass, which represents a variety of realistic changes in working condition for a suspension system supporting sensitive instrumentation. While the mass of the host structure remains $m_2 = 1.029$, the suspended mass is varied by connecting blocks of brass to the top bearing. In this way, three suspended masses are realized: $[m_1^{(1)}, m_1^{(2)}, m_1^{(3)}] = [0.347, 0.6, 0.847]$ kg. The RMS of excitation levels for experimental and analytical results are the same as those employed in the prior section. For the analytical results, six values of suspended mass are chosen: $[m_1^{(1)}, m_1^{(2)}, \ldots, m_1^{(6)}] = [0.347, 0.6, 0.847, 2.0, 4.0, 6.0]$ kg, where the final three values are greater than were able to be evaluated experimentally. The bistable suspension damping values in the experiment and analysis are chosen to be the smallest cases used in the prior section, respectively.

Fig. 8(a and b) presents experimental and analytical transmissibilities, respectively, as the suspended mass is varied. There is good qualitative agreement between analytical and measured data and both results indicate that the frequency bandwidths leading to inter-well response do not vary corresponding to change of the suspended mass. The experimental and analytical results by investigating the lighter suspended masses $m_1^{(1)}$, $m_1^{(2)}$ and $m_1^{(3)}$ show that the maximum $|T|$ is decreased as the suspended mass is increased. Analytical results in Fig. 8(b) show that when the suspended mass becomes greater than the frame mass, shown by $[m_1^{(4)}, m_1^{(5)}, m_1^{(6)}]$, the transmissibility continues to reduce. While the trend shows that large suspended mass is beneficial to achieve small vibration transmission in the resonance bandwidth, too heavy of suspended load may lead to large deflection of the bistable interface when the suspension is subjected to high body force, for example inertial force due to aerospace vehicle launch acceleration. In practice, supporting too large of mass may not

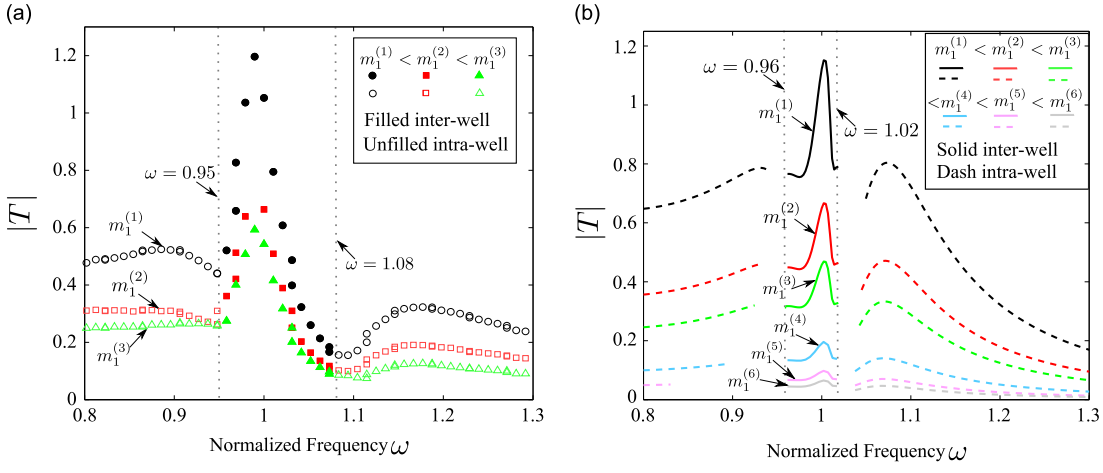

Fig. 8. (a) Experimental and (b) analytical transmissibility $|T|$ corresponding to suspended mass variation.

satisfy static deflection constraints of the bistable spring. Therefore, the trade-off between bistable spring deflection constraints and suspension performance should be considered to appropriately support the suspended mass and ensure the operational safety of suspension system.

9. Conclusion

Performance of a bistable suspension when attached to a flexible host structure is investigated as means to enhance operation safety by exploiting the dynamic stabilization phenomenon. In this way, the bistable suspension avoids inducing the detrimental resonance adjacent to the roll-off frequency band that otherwise compromises the safety of a comparable linear suspension. That is, when the excitation frequency shifts from the roll-off band and approaches the resonance bandwidth, the vibration may not be amplified, leading to significant enhancement of operational safety. Through analytical, numerical, and experimental investigations, this study details design and operation methods to ensure beneficial single periodic response around this resonance bandwidth for reduction in vibration transmission. Numerical and experimental results validate analytical predictions for a variety of systematic variations in excitation and system parameters critical in suspension systems. The findings suggest that moderate excitation level and appropriately low damping are key to favorable design and implementation of the bistable suspension. Lastly, a trade-off exists between bistable spring deflection constraints and performance improvement in terms of the suspended mass with respect to the host structure apparent mass; therefore, operational safety of the suspension system may be ensured by designing the bistable suspension in light of the anticipated range of supported masses.

Acknowledgments

This work is supported in part by a China Scholarship Council Grant no. 201206020092 and the University of Michigan Collegiate Professorship fund.

References

[1] D. Karnopp, Active and semi-active vibration isolation, *Journal of Vibration and Acoustics* 117 (1995) 177–185.
[2] A. Preumont, K. Seto, *Active Control of Structures*, John Wiley & Sons, Ltd, Chichester, UK, 2008.
[3] T. Yoshimura, A. Kume, M. Kurimoto, J. Hino, Construction of an active suspension system of a quarter car model using the concept of sliding mode control, *Journal of Sound and Vibration* 239 (2001) 187–199.
[4] H. Du, K.Y. Sze, J. Lam, Semi-active H∞ control of vehicle suspension with magneto-rheological dampers, *Journal of Sound and Vibration* 283 (2005) 981–996.
[5] Y.-T. Choi, N.M. Wereley, Y.-S. Jeon, Semi-active vibration isolation using magnetorheological isolators, *Journal of Aircraft* 42 (2005) 1244–1251.
[6] G.J. Hiemenz, W. Hu, N.M. Wereley, Semi-active magnetorheological helicopter crew seat suspension for vibration isolation, *Journal of Aircraft* 45 (2008) 945–953.
[7] C. Chen, W.-H. Liao, A self-sensing magnetorheological damper with power generation, *Smart Materials and Structures* 21 (2012) 025014.
[8] B. Sapiński, Experimental study of a self-powered and sensing MR-damper-based vibration control system, *Smart Materials and Structures* 20 (2011) 105007.
[9] Y.-T. Choi, H.J. Song, N.M. Wereley, Semi-active isolation system using self-powered magnetorheological dampers, in: N.M. Wereley (Ed.), *Magnetorheology: Advances and Applications*, Royal Society of Chemistry, RSC Smart Materials, Cambridge, UK2013, pp. 288–306.
[10] D.L. Platus, Negative-stiffness-mechanism vibration isolation systems, *Proceedings of SPIE 1619 Vibration Control in Microelectronics, Optics, and Metrology* (1992) 44–54.
[11] A. Carrella, M.J. Brennan, T.P. Waters, V. Lopes Jr., Force and displacement transmissibility of a nonlinear isolator with high-static-low-dynamic-stiffness, *International Journal of Mechanical Sciences* 55 (2012) 22–29.
[12] R.L. Harne, K.W. Wang, A review of the recent research on vibration energy harvesting via bistable systems, *Smart Materials and Structures* 22 (2013) 023001.
[13] Y. Kim, S.Y. Lee, S.-Y. Kim, Experimental observation of dynamic stabilization in a double-well Duffing oscillator, *Physics Letters A* 275 (2000) 254–259.
[14] Z. Wu, R.L. Harne, K.W. Wang, Excitation-induced stability in a bistable Duffing oscillator: analysis and experiments, *Journal of Computational and Nonlinear Dynamics* (2014), http://dx.doi.org/10.1115/1.4026974. (in press).
[15] K. Yang, R.L. Harne, K.W. Wang, H. Huang, Investigation of a bistable dual-stage vibration isolator under harmonic excitation, *Smart Materials and Structures* 23 (2014) 045033.
[16] L.N. Virgin, *Introduction to Experimental Nonlinear Dynamics: A Case Study in Mechanical Vibration*, Cambridge University Press, Cambridge, UK, 2000.
[17] W.-Y. Tseng, J. Dugundji, Nonlinear vibrations of a buckled beam under harmonic excitation, *Journal of Applied Mechanics* 38 (1971) 467–476.
[18] R.L. Harne, M. Thota, K.W. Wang, Concise and high-fidelity predictive criteria for maximizing performance and robustness of bistable energy harvesters, *Applied Physics Letters* 102 (2013) 053903.
[19] Z. Wu, R.L. Harne, K.W. Wang, Energy harvester synthesis via coupled linear-bistable system with multistable dynamics, *Journal of Applied Mechanics* 81 (2014) 061005.